

Polarized thermal emission from dust in a galaxy at redshift 2.6

J. E. Geach¹, E. Lopez-Rodriguez², M. J. Doherty¹, Jianhang Chen³, R. J. Ivison³, G. J. Bendo⁴, S. Dye⁵, K. E. K. Coppin¹

¹Centre for Astrophysics Research, School of Physics, Engineering and Computer Science, University of Hertfordshire, College Lane, Hatfield AL10 9AB, UK

²Kavli Institute for Particle Astrophysics & Cosmology (KIPAC), Stanford University, Stanford, CA 94305, USA

³European Southern Observatory, Karl-Schwarzschild-Strasse 2, D-85748 Garching, Germany

⁴UK ALMA Regional Centre Node, Jodrell Bank Centre for Astrophysics, Department of Physics and Astronomy, The University of Manchester, Oxford Road, Manchester M13 9PL, UK

⁵School of Physics and Astronomy, University of Nottingham, University Park, Nottingham NG7 2RD, UK

Magnetic fields are fundamental to the evolution of galaxies, playing a key role in the astrophysics of the interstellar medium (ISM) and star formation. Large-scale ordered magnetic (B) fields have been mapped in the Milky Way and nearby galaxies^{1,2}, but it is not known how early in the Universe such structures form³. Here we report the detection of linearly polarized thermal emission from dust grains in a strongly lensed, intrinsically luminous galaxy that is forming stars at a rate more than a thousand times that of the Milky Way at redshift 2.6, within 2.5 Gyr of the Big Bang^{4,5}. The polarized emission arises from the alignment of dust grains with the local magnetic field^{6,7}. The median polarization fraction is of order one per cent, similar to nearby spiral galaxies⁸. Our observations support the presence of a 5 kiloparsec-scale ordered B -field with a strength of around $500\mu\text{G}$ or lower, orientated parallel to the molecular gas disc. This confirms that such structures can be rapidly formed in galaxies, early in cosmic history.

We observed the lensed galaxy 9io9⁴ with the Atacama Large Millimeter/Submillimeter Array (ALMA) at a representative frequency of 242 GHz (equivalent to a wavelength of approximately $350\mu\text{m}$ in the rest-frame of the galaxy) to record the dust continuum emission averaged over a total bandwidth of 7.5 GHz. The set of XX , YY , XY and YX linear polarization parameters recorded in full polarization mode allow measurement of the Stokes parameters Q and U , yielding the total linearly polarized intensity, $PI = \sqrt{Q^2 + U^2}$, and position angle (PA) of polarized emission $\chi = 0.5 \arctan(U/Q)$. The root mean squared sensitivity of the observations is $\sigma_I = 47\mu\text{Jy beam}^{-1}$ and $\sigma_Q \sim \sigma_U = 9\mu\text{Jy beam}^{-1}$. In Figure 1 we present image plane maps of the total intensity I , Stokes Q and U , and polarized intensity PI . The polarization angle χ is rotated by 90 degrees to show the plane-of-the-sky B -field orientation (χ_B). We mea-

36 sure an image plane integrated flux density of $I = 62$ mJy, integrated polarization fraction of
 37 $P = 0.6 \pm 0.1\%$, where $P = PI/I$, and B -field orientation of $\chi_B = (-0.7 \pm 1.4)$ degrees. The
 38 mean of the distribution of polarization fractions and B -field orientations is $\langle P \rangle = 0.6 \pm 0.3\%$
 39 and $\langle \chi_B \rangle = (0.8 \pm 18.3)$ degrees, respectively. Note that the uncertainties are the dispersion of
 40 the distribution of individual measurements within the galaxy, not the accuracy in the polarization
 41 measurement (Methods).

42 Using the lens model derived from previous high-resolution millimetre continuum emission
 43 and optical *Hubble Space Telescope* imaging, the source plane CO(4–3) emission, tracing the
 44 cold molecular gas reservoir, has been shown to be well-modelled by a rotating disc of maximum
 45 radius 2.6 kpc, inclined by approximately 50 degrees to the line of sight, with a position angle
 46 (PA) on the sky of approximately 5 degrees East of North^{4,5}. With this model as a constraint, we
 47 explore what source plane B -field configurations are consistent with the image plane polarization
 48 observations. The most likely source plane configuration is a large-scale ordered B -field orientated
 49 $\chi_B = 5_{-10}^{+5}$ degrees east of north with an extent matching that of the CO emission (Figure 2). This
 50 result implies the presence of a 5 kpc-scale galactic ordered magnetic field orientated parallel to
 51 the molecular gas-rich disc. Angular variations of χ_B across the galaxy present in the image plane
 52 maps, corresponding to scales of 600 pc in the source plane, can be explained by the low signal-
 53 to-noise ratio and beam effects (Methods). This result implies that the introduction of a random
 54 B -field component with an angular variation of ± 5 degrees in addition to the large-scale ordered B -
 55 field is also consistent with the observations. We currently lack the sensitivity and resolution to map
 56 the configuration of the B -field strength at scales ~ 100 pc where structure related to turbulence can
 57 start to be resolved. The observed B -field configuration parallel to the disc is consistent with the
 58 galactic B fields measured in local spiral galaxies observed at far-infrared and radio wavelengths^{1,2}.
 59 Note that our far-infrared polarimetric observations trace a density-weighted average B -field in the
 60 cold and dense ISM, rather than a volume average B -field in the warm and diffuse ISM by radio
 61 polarimetric observations.

62 The mean and integrated polarization fractions of 9io9 are consistent with the $P \sim 0.8\%$
 63 level measured in nearby spiral and starburst galaxies at wavelengths of 53–214 μm^2 . The ob-
 64 servations presented here are sensitive to polarized emission beyond this range, pushing into the
 65 Rayleigh-Jeans tail of the thermal emission spectrum at $\lambda_{\text{rest}} = 350 \mu\text{m}$. In recent models of diffuse
 66 interstellar dust, the polarization fraction, P , is independent of wavelength across 200–2000 μm ,
 67 consistent with observations of Galactic dust emission². Observations of local starburst galaxies
 68 show that P only varies by 0.4 per cent over the 50–150 μm range, with an increase of up to ~ 1
 69 per cent towards 214 μm^2 . We therefore conclude that 9io9 has a polarization level similar to lo-
 70 cal star-forming discs and starburst galaxies, with a key difference being the order-of-magnitude
 71 difference in gas mass and star-formation rate, with the disc of 9io9 being close to molecular gas

72 dominated, contrasted with the $f_{\text{gas}} \approx 10$ per cent gas fractions of local star-forming discs⁹.

73 The large-scale ordered magnetic fields that exist in massive disc galaxies in the local Uni-
74 verse is thought to arise through the amplification of seed fields, and this has been predicted
75 to occur on relatively short cosmological timescales, of order 1 Gyr^{10–12}. Weak seed fields (as
76 low as $B \sim 10^{-20}$ G) could be formed in protogalaxies either through trapping of a cosmolog-
77 ical field, possibly primordial in nature, or through the battery effect following the onset of star
78 formation^{13–16}. Although turbulent gas motions in discs can reduce net polarization if they im-
79 part a strong turbulent component to the B -field¹⁷, recent theoretical models of the formation of
80 galactic-scale magnetic fields invoke turbulence in the ISM as the origin of a ‘small-scale’ dy-
81 namo that can rapidly amplify the weak seed fields to μG levels^{12,18,19}. This small-scale dynamo is
82 mainly driven by supernova explosions with coherence lengths of order 50–100 pc, but turbulence
83 can be injected into the ISM on multiple scales through disc instabilities and feedback effects, in-
84 cluding stellar winds and outflows driven by radiation pressure, supernova explosions, and large
85 scale outflows from an active galactic nucleus.

86 The average turbulent velocity component of the disc of 9io9, determined from kinematic
87 modelling of the CO emission, is $\sigma_v \approx 70 \text{ km s}^{-1}$ and the star-formation rate density exceeds
88 $100 M_{\odot} \text{ yr}^{-1} \text{ kpc}^{25}$. The high dense gas fraction of the molecular reservoir – as traced by the ra-
89 tio of CO(4–3)/C I(1–0) emission – is also consistent with the injection of supersonic turbulence,
90 which plays a key role in shaping the lognormal probability distribution function of the molecular
91 gas density²⁰. There is also tentative evidence of stellar feedback in action through the broad lines
92 of dense gas tracers⁵. Finally, one expects a high cosmic ray flux density in the ISM of 9io9, com-
93 mensurate with the high star-formation rate density, and this too could serve to amplify magnetic
94 fields. Therefore, 9io9 likely has the conditions required to rapidly amplify any weak seed fields via
95 the small-scale dynamo effect, with amplification occurring on scales up to and including the full
96 star-forming disc. Assuming equipartition between the turbulent kinetic and magnetic energies, we
97 estimate an upper-limit of the equipartition turbulent B -field strength of $514 \mu\text{G}$ (Methods). This is
98 comparable to the estimated turbulent B -field strength of $305 \pm 15 \mu\text{G}$ within the central kiloparsec
99 of the starburst region of M82 also using FIR polarimetric observations²¹. This indicates that the
100 starburst activity of 9io9 could be driving the amplification of B -fields across the disc.

101 Feedback-induced turbulence is a route to accelerating the growth of the seed fields, but
102 to produce the ordered field on the kpc-scales observed requires a mean-field dynamo^{14,22}. This
103 mean-field dynamo can be achieved through the rapid differential rotation of the gas disc, and
104 this provides a mechanism for the ordering of an amplified B -field driven by star formation and
105 stellar feedback processes. 9io9 is turbulent, intensely star-forming and rapidly rotating ($v_{\text{max}} \approx$
106 300 km s^{-1}). This suggests that rather than an episode of violent feedback priming a large-scale but

107 turbulent field that later evolves into an ordered field during a period of relative quiescence¹⁹, the
108 small-scale and mean-field dynamo mechanisms operate in tandem. We estimate that the mean-
109 field dynamo in 9io9 has not yet had time to maintain or amplify the B -field (Methods). This
110 implies that the intense starburst is most important in amplifying the galactic field at $z = 2.6$.
111 We postulate that this ‘dual dynamo’ might be the common mode by which galactic-scale ordered
112 magnetic fields are established in young gas-rich, turbulent galaxies in the early Universe.

113 Coherent magnetic fields consistent with the mean-field dynamo have been observed at $z =$
114 0.4 via Faraday rotation of a background polarized radio source³ (note that such observations are
115 not possible for 9io9). Magnetic fields are already known to be present in the environment around
116 normal galaxies at $z \approx 1$ as revealed by the association of Mg II absorption systems along quasar
117 sightlines that exhibit Faraday rotation²³, and indirectly through the existence of radio synchrotron
118 emission from star-forming galaxies. However, mapping the B -fields in individual galaxies at high
119 redshift has so-far proven challenging. Our observations show that the polarized emission from
120 magnetically aligned dust grains is a powerful tool to trace the B -fields of the cold and dense ISM
121 in high redshift galaxies.

122 9io9 is a particularly luminous example of a population of dusty star-forming galaxies in the
123 early Universe that contribute a significant portion of the cosmic infrared background (CIB). If
124 the one per cent level of polarization detected in 9io9 is representative of the general population
125 of dusty star-forming galaxies²⁴ then routine detection and mapping of magnetic fields in galaxies
126 at high redshift is feasible (i.e., in integration times of less than 24 hr) even in unlensed systems
127 with ALMA. This offers a new window to characterise the physical conditions of the ISM in
128 galaxies when galaxy growth was at its maximum, and will enable a better understanding the role
129 of magnetic fields in shaping the early stages of galaxy evolution. The strength of the galactic
130 magnetic field in local spiral galaxies is of order $10 \mu\text{G}$ ¹, and up to an order of magnitude higher in
131 starbursts⁸. Without resolving the polarization field in 9io9 below 100 pc scales it is not possible to
132 reliably estimate the B -field strength using dust polarization observations. Nevertheless, given the
133 injection of kinetic turbulence driven by stellar feedback we estimate the strength of the B -field in
134 9io9 to be likely greater than that of local spiral galaxies, but similar to that of the central regions
135 of nearby starburst galaxies (Methods).

136 Finally, these observations imply the CIB itself may be weakly polarized^{24,25}. Although mis-
137 alignments of galaxies along the line of sight will serve to reduce the net polarization of the CIB,
138 if the orientation of discs that host large scale ordered B -fields is correlated on large scales due to
139 tidal alignments²⁶, then a polarization signal could remain, and therefore fluctuations in the polar-
140 ization intensity of the CIB could be used as a new probe of the physics of structure formation²⁵.
141 This has consequences for cosmological experiments that seek to derive information on primordial

142 conditions from observations of the polarization of the cosmic microwave background (CMB), es-
143 pecially if a curl component is present in the CIB polarization field^{25,27}. A polarized component
144 of the CIB at millimeter wavelengths, of extragalactic origin and dominated by emission at $z \approx 2$
145 and with a power spectrum that is driven by large scale structure at this epoch, will be a subtle but
146 important foreground for future precision CMB experiments to contend with.

147 **Acknowledgements** This paper makes use of the following ALMA data: ADS/JAO.ALMA#021.1.01461.S.
148 ALMA is a partnership of ESO (representing its member states), NSF (USA) and NINS (Japan), together
149 with NRC (Canada), MOST and ASIAA (Taiwan), and KASI (Republic of Korea), in cooperation with the
150 Republic of Chile. The Joint ALMA Observatory is operated by ESO, AUI/NRAO and NAOJ. J.E.G. and
151 M.D. acknowledge support from the Royal Society.

152 **Author Contributions** JEG led the proposal to obtain the data and designed the observations; JEG and
153 GJB reduced the data; JEG and ELR performed the analysis and all authors contributed to the manuscript.

- 155 1. Beck, R., Chamandy, L., Elson, E. & Blackman, E. G. Synthesizing Observations and Theory
156 to Understand Galactic Magnetic Fields: Progress and Challenges. *Galaxies* **8**, 4 (2019).
- 157 2. Lopez-Rodriguez, E. *et al.* Extragalactic Magnetism with SOFIA (SALSA Legacy Program):
158 The Magnetic Fields in the Multiphase Interstellar Medium of the Antennae Galaxies. *The*
159 *Astrophysical Journal Letters* **942**, L13 (2022).
- 160 3. Mao, S. A. *et al.* Detection of microgauss coherent magnetic fields in a galaxy five billion
161 years ago. *Nature Astronomy* **1**, 621–626 (2017).
- 162 4. Geach, J. E. *et al.* The Red Radio Ring: a gravitationally lensed hyperluminous infrared radio
163 galaxy at $z = 2.553$ discovered through the citizen science project Space Warps. *Monthly*
164 *Notices of the Royal Astronomical Society* **452**, 502–510 (2015).
- 165 5. Geach, J. E., Ivison, R. J., Dye, S. & Oteo, I. A Magnified View of Circumnuclear Star
166 Formation and Feedback around an Active Galactic Nucleus at $z = 2.6$. *Astrophys. J. Lett.*
167 **866**, L12 (2018).
- 168 6. Hoang, T. & Lazarian, A. Radiative torque alignment: essential physical processes. *Monthly*
169 *Notices of the Royal Astronomical Society* **388**, 117–143 (2008).
- 170 7. Andersson, B.-G., Lazarian, A. & Vaillancourt, J. E. Interstellar dust grain alignment. *Annual*
171 *Review of Astronomy and Astrophysics* **53**, 501–539 (2015).
- 172 8. Lopez-Rodriguez, E. *et al.* Extragalactic Magnetism with SOFIA (SALSA Legacy Program).
173 IV. Program Overview and First Results on the Polarization Fraction. *Astrophys. J.* **936**, 92
174 (2022).

- 175 9. Saintonge, A. & Catinella, B. The Cold Interstellar Medium of Galaxies in the Local Universe.
176 ARA&A **60**, 319–361 (2022).
- 177 10. Beck, R., Poezd, A. D., Shukurov, A. & Sokoloff, D. D. Dynamos in evolving galaxies.
178 Astron. Astrophys. **289**, 94–100 (1994).
- 179 11. Brandenburg, A. & Subramanian, K. Astrophysical magnetic fields and nonlinear dynamo
180 theory. Phys. Rep. **417**, 1–209 (2005).
- 181 12. Schober, J., Schleicher, D. R. G. & Klessen, R. S. Magnetic field amplification in young
182 galaxies. Astron. Astrophys. **560**, A87 (2013).
- 183 13. Biermann, L. Über den Ursprung der Magnetfelder auf Sternen und im interstellaren Raum
184 (miteinem Anhang von A. Schlüter). *Zeitschrift Naturforschung Teil A* **5**, 65 (1950).
- 185 14. Beck, R., Brandenburg, A., Moss, D., Shukurov, A. & Sokoloff, D. Galactic Magnetism:
186 Recent Developments and Perspectives. ARA&A **34**, 155–206 (1996).
- 187 15. Kulsrud, R. M. & Zweibel, E. G. On the origin of cosmic magnetic fields. *Reports on Progress*
188 *in Physics* **71**, 046901 (2008).
- 189 16. Subramanian, K. From Primordial Seed Magnetic Fields to the Galactic Dynamo. *Galaxies* **7**,
190 47 (2019).
- 191 17. Lee, H. M. & Draine, B. T. Infrared extinction and polarization due to partially aligned
192 spheroidal grains: models for the dust toward the BN object. *Astrophys. J.* **290**, 211–228
193 (1985).
- 194 18. Rieder, M. & Teyssier, R. A small-scale dynamo in feedback-dominated galaxies as the origin
195 of cosmic magnetic fields - I. The kinematic phase. *Mon. Not. R. Astron. Soc.* **457**, 1722–1738
196 (2016).
- 197 19. Rieder, M. & Teyssier, R. A small-scale dynamo in feedback-dominated galaxies - III. Cos-
198 mological simulations. *Mon. Not. R. Astron. Soc.* **472**, 4368–4373 (2017).
- 199 20. Padoan, P. & Nordlund, Å. The Stellar Initial Mass Function from Turbulent Fragmentation.
200 *Astrophys. J.* **576**, 870–879 (2002).
- 201 21. Lopez-Rodriguez, E., Guerra, J. A., Asgari-Targhi, M. & Schmelz, J. T. The Strength and
202 Structure of the Magnetic Field in the Galactic Outflow of Messier 82. *Astrophys. J.* **914**, 24
203 (2021).
- 204 22. Ruzmaikin, A., Sokolov, D. & Shukurov, A. Magnetism of spiral galaxies. *Nature* **336**,
205 341–347 (1988).

- 206 23. Bernet, M. L., Miniati, F., Lilly, S. J., Kronberg, P. P. & Dessauges-Zavadsky, M. Strong
207 magnetic fields in normal galaxies at high redshift. *Nature* **454**, 302–304 (2008).
- 208 24. Bonavera, L., González-Nuevo, J., De Marco, B., Argüeso, F. & Toffolatti, L. Statistics of
209 the fractional polarization of extragalactic dusty sources in Planck HFI maps. *Mon. Not. R.*
210 *Astron. Soc.* **472**, 628–635 (2017).
- 211 25. Feng, C. & Holder, G. Polarization of the Cosmic Infrared Background Fluctuations. *Astro-*
212 *phys. J.* **897**, 140 (2020).
- 213 26. Hirata, C. M. & Seljak, U. Intrinsic alignment-lensing interference as a contaminant of cosmic
214 shear. *Phys. Rev. D* **70**, 063526 (2004).
- 215 27. Lagache, G., Béthermin, M., Montier, L., Serra, P. & Tucci, M. Impact of polarised extra-
216 galactic sources on the measurement of CMB B-mode anisotropies. *Astron. Astrophys.* **642**,
217 A232 (2020).

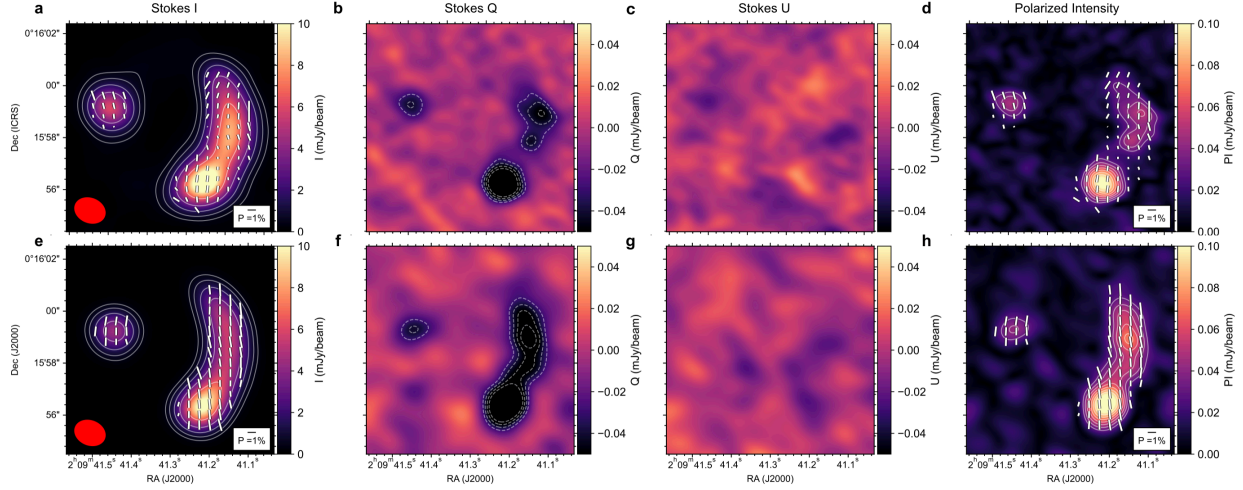


Figure 1: **The magnetic field orientation of the gravitationally lensed galaxy 9io9 at $z=2.553$.** (a-d), ALMA 242 GHz polarimetric observations of the Stokes I , Q , and U parameters, and the polarized intensity PI . The synthetic beam of the observations ($1.2'' \times 0.9''$, $\theta = 68$ degrees) is shown as the red ellipse, lower left. The B -field orientation is indicated by white lines displayed at the Nyquist sampling, with line lengths proportional to the polarization fraction. (e-h), Synthetic polarimetric observations using a constant B -field configuration in the source plane. Contours indicate signal-to-noise: for Stokes I , the contours increase as $\sigma_I \times 2^{3,4,5,\dots}$. For Stokes Q and U , and PI , the contours start at 3σ and increase in steps of 1σ .

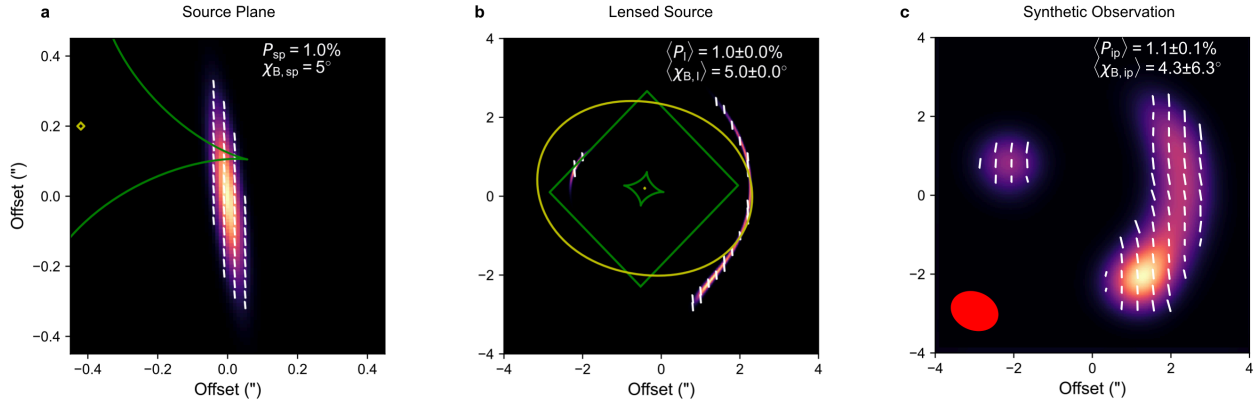


Figure 2: **Source plane configuration of the magnetic field and lensing model.** (a) Source plane intensity and field orientation. (b) Lensed source plane image. (c) Synthetic observations with the synthetic beam size ($1.2'' \times 0.9''$, $\theta = 68$ degrees) indicated by the red ellipse. The B -field orientation is indicated by white lines with lengths proportional to the polarization fraction. The median and root mean squared values of the polarization fraction and B -field orientation are indicated top right. The caustics in the source plane and image plane are shown as green and yellow lines respectively.